Nuclear Membrane Dynamics and Reassembly in Living Cells: Targeting of an Inner Nuclear Membrane Protein in Interphase and Mitosis

Jan Ellenberg,* Eric D. Siggia,‡ Jorge E. Moreira,* Carolyn L. Smith,§ John F. Presley,* Howard J. Worman,‖ and Jennifer Lippincott-Schwartz*

*Cell Biology and Metabolism Branch, National Institute of Child Health and Human Development, National Institutes of Health (NIH), Bethesda, Maryland 20892; ‡Department of Physics, Cornell University, Ithaca, New York 14853; §Light Imaging Facility, National Institute of Neurological Disorders and Stroke, NIH, Bethesda, Maryland 20892; and ‖Departments of Medicine and of Anatomy and Cell Biology, College of Physicians and Surgeons, Columbia University, New York 10032

Abstract. The mechanisms of localization and retention of membrane proteins in the inner nuclear membrane and the fate of this membrane system during mitosis were studied in living cells using the inner nuclear membrane protein, lamin B receptor, fused to green fluorescent protein (LBR–GFP). Photobleaching techniques revealed the majority of LBR–GFP to be completely immobilized in the nuclear envelope (NE) of interphase cells, suggesting a tight binding to heterochromatin and/or lamins. A subpopulation of LBR–GFP within ER membranes, by contrast, was entirely mobile and diffused rapidly and freely ($D = 0.41 \pm 0.1\ \mu m^2/s$). High resolution confocal time-lapse imaging in mitotic cells revealed LBR–GFP redistributing into the interconnected ER membrane system in prometaphase, exhibiting the same high mobility and diffusion constant as observed in interphase ER membranes. LBR–GFP rapidly diffused across the cell within the membrane network defined by the ER, suggesting the integrity of the ER was maintained in mitosis, with little or no fragmentation and vesiculation. At the end of mitosis, nuclear membrane reformation coincided with immobilization of LBR–GFP in ER elements at contact sites with chromatin. LBR–GFP–containing ER membranes then wrapped around chromatin over the course of 2–3 min, quickly and efficiently compartmentalizing nuclear material. Expansion of the NE followed over the course of 30–80 min. Thus, selective changes in lateral mobility of LBR–GFP within the ER/NE membrane system form the basis for its localization to the inner nuclear membrane during interphase. Such changes, rather than vesiculation mechanisms, also underlie the redistribution of this molecule during NE disassembly and reformation in mitosis.

MEMBRANES of the nuclear envelope (NE)[1] serve to compartmentalize the nucleus of higher eukaryotic cells. They are in direct continuity with the ER and consist of two concentric bilayers that are joined only at nuclear pore complexes (Fig. 1 *A*). The outer nuclear membrane shares its proteins and functional properties with the ER, whose lumen is continuous with the perinuclear space (Fig. 1 *A*). The inner nuclear membrane has unique characteristics. It contains a distinct set of membrane proteins, including lamin B receptor (LBR; Worman et al., 1988, 1990; Ye and Worman, 1994), LAP1C (Martin et al., 1995), LAP2 (Furukawa et al., 1995), and emerin (Bione et al., 1994; Nagano et al., 1996). Their functions include providing attachment sites for heterochromatin and the nuclear lamina, the latter of which is a meshwork of intermediate filaments that associates with interphase chromatin and lines the inner nuclear membrane (for review see Gerace and Burke, 1988). Molecular interactions between inner nuclear membrane proteins, chromatin, and the lamina are widely recognized to be crucial for the structural maintenance of the NE, the higher level organization of chromosomes during interphase, and NE disassembly and reformation during mitosis (Gerace and Burke, 1988; Marshall and Wilson, 1997). How membrane proteins are targeted to and retained in the inner

Address all correspondence to Jennifer Lippincott-Schwartz, Cell Biology and Metabolism Branch, NICHD, NIH, Bethesda, MD 20892. Tel.: (301) 402-1010. Fax: (301) 402-0078. e-mail: jlippin@helix.nih.gov

1. *Abbreviations used in this paper*: FLIP, fluorescence loss in photobleaching; FRAP, fluorescence recovery after photobleaching; GFP, green fluorescent protein; LBR, lamin B receptor; NE, nuclear envelope.

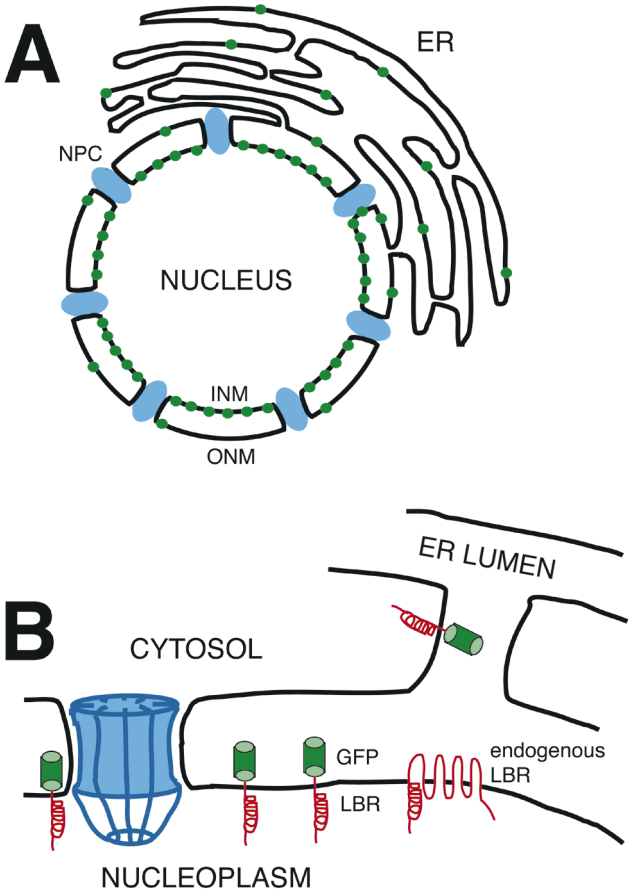

Figure 1. Schematic overview of nuclear architecture and LBR–GFP topology. (*A*) NE and ER membrane continuities. Nuclear pore complexes (*NPC*) are depicted in blue, and a protein targeted to the inner nuclear membrane (*INM*) in green. Note its equal and random distribution in ER and outer nuclear membrane (*ONM*) and its concentration in the INM. Possible diffusion through the pore membrane is shown in one case. (*B*) Detail of *A* showing predicted topology of full-length LBR (*endogenous*) and LBR–GFP. LBR–GFP contains the NH_2-terminal nucleoplasmic tail as well as the first transmembrane span of full-length LBR (amino acids 1–238), resulting in a lumenal GFP localization.

nuclear membrane and their fate during mitosis is therefore central to understanding NE function.

The primary model for how integral membrane proteins become localized to the inner nuclear membrane after their synthesis in the ER proposes their lateral diffusion through the proteolipid bilayer of the ER into the outer nuclear membrane, diffusion through the nuclear pore membrane, and then diffusion into the inner membrane (Smith and Blobel, 1993; Soullam and Worman, 1993, 1995). In this model, the proteins are subsequently immobilized by binding to nucleoplasmic ligands or multimerization. Indirect evidence favors this view over alternatives that have been proposed, such as sorting to precursor structures at the end of mitosis. Such evidence includes data showing (*a*) the exchange of an inner nuclear membrane protein between two nuclei during interphase in heterokaryons (Powell and Burke, 1990), (*b*) that small viral envelope proteins have free access to the inner nuclear membrane without being specifically retained there (Bergman and Singer, 1983; Torrisi et al., 1987, 1989), and (*c*) that membrane proteins with cytosolic/nucleoplasmic domains greater than 70 kD fail to localize to the inner nuclear membrane (Soullam and Worman, 1995). The latter finding is presumably due to a size constraint imposed by the lateral channel diameter of the nuclear pore complex on diffusion through the pore membrane (Hinshaw et al., 1992; Akey, 1995). Despite this suggestive evidence for a diffusion/retention mechanism for protein targeting to the inner nuclear membrane, data on the diffusional mobility of NE membrane proteins in the ER and within the inner nuclear membrane has heretofore been lacking.

NE disassembly and reformation during mitosis also requires membrane targeting and localization of NE membrane proteins, but it has been generally assumed that the relevant mechanism is distinct from that which operates during interphase. The prevailing view is that nuclear membranes fragment into tubules and vesicles that are released into the cytoplasm when the lamina is depolymerized during prophase. This view is supported by ultrastructural work (Robbins and Gonatas, 1964; Wasserman and Smith, 1978; Zeligs and Wollman, 1979), as well as by in vitro data derived from cell-free systems (Lohka, 1988; Newport and Dunphy, 1992; Buendia and Courvalin, 1997). Mechanistically, NE breakdown has been shown to be mediated by mitotic kinase–induced phosphorylation of many NE protein components, such as lamins (Gerace and Blobel, 1980), inner nuclear membrane proteins (Pfaller et al., 1991; Courvalin et al., 1992; Foisner and Gerace, 1993), and nucleoporins (Macauley et al., 1995; Favreau et al., 1996), disrupting protein–protein interactions necessary for maintaining NE integrity.

NE reformation is thought to be the reverse of disassembly, with precursor vesicles containing NE membrane proteins that are dispersed throughout the cytoplasm now targeting and binding to decondensing chromatin followed by coordinated fusion and sorting of proteins within these vesicles (Wiese and Wilson, 1993; Marshall and Wilson, 1997). Such a mechanism requires a specific machinery for regulating and mediating vesicle budding and fusion events and has been proposed to share properties of vesicular transport in the secretory pathway (Rothman and Wieland, 1996; Wilson and Wiese, 1996). The vesiculation model also implies segregation of NE and ER membranes during mitosis, since mitotic ER membranes remain as an intact tubular cisternal network in many cells types (Porter and Machado, 1960; Zatespina et al., 1977; Waterman-Storer et al., 1993; Ioshii et al., 1995; Terasaki, M., and P. Peters, personal communications).

New techniques of fluorescently tagging proteins (Chalfie et al., 1994) now make it possible to study NE membrane dynamics in living cells. To test the current models for protein targeting and localization to the NE membranes in interphase and during reformation after mitosis, we have used a well-characterized protein of the inner nuclear membrane, human LBR, tagged with green fluorescent protein (GFP). LBR is a type II membrane protein with eight putative transmembrane segments whose NH_2 terminus faces the cytosol/nucleoplasm (Fig. 1 *B*). This domain of LBR binds in vitro to B-type lamins and phage λ DNA (Ye and Worman, 1994), and to human homologues

of *Drosophila* heterochromatin protein HP-1 (Ye and Worman, 1996; Ye et al., 1997). Data from reconstituted liposomes and reassembly assays using sea urchin eggs suggests that LBR is the major chromatin docking protein in NE membranes (Pyrpasopoulou et al., 1996; Collas et al., 1996). During mitosis, LBR is a substrate for $p34^{cdc2}$ and other kinases (Courvalin et al., 1992; Nikolakaki et al., 1997). Changes in its phosphorylation state, therefore, can potentially disrupt association with the lamina and heterochromatin, as has been proposed for other inner nuclear membrane proteins (Pfaller et al., 1991; Foisner and Gerace, 1993).

In this study, we use fluorescence recovery after photobleaching techniques (FRAP) to demonstrate that LBR–GFP diffuses rapidly and freely within ER membranes of interphase cells. Once localized to the inner nuclear membrane, however, LBR–GFP becomes completely immobilized, suggesting a tight binding to heterochromatin and/or the lamina. This provides important support to the diffusion/retention model for inner nuclear membrane localization during interphase. At the same time, our findings in mitotic cells are contrary to the vesiculation model for NE membrane disassembly and reassembly. Instead, it appears that the same basic processes at work during interphase can also explain mitotic localization of inner nuclear membrane proteins. Through changes in their diffusional mobility, inner nuclear membrane proteins redistribute into ER membranes during NE disassembly and localize back at the end of mitosis by a process of immobilization within ER elements that contact and then envelope chromosomal material.

Materials and Methods

Cells and DNA Constructs

COS-7 cells (American Type Culture Collection, Rockville, MD) were used in all experiments. They were grown on No. 1 glass coverslips at 37°C in Dulbecco's Minimal Essential Medium supplemented with 10% FCS, 2 mM glutamine, 100 μg/ml penicillin, 100 U/ml streptomycin, and 25 mM Hepes-KOH, pH 7.3 (complete medium). Cells were imaged live on temperature-controlled microscopes at 37°C. Mitotic cells were identified in a population of expressing cells, rather than through cell cycle synchronization procedures. The LBR–GFP fusion used in this study includes the first 238 amino acids of human LBR (Ye and Worman, 1994) fused to the F64L, S65T, H231L variant of the GFP with a four–amino acid spacer (PVAT) in the expression vector pEGFP-N1 (CLONTECH Laboratories, Palo Alto, CA) and was generated by standard procedures (Sambrook et al., 1989). Cells were transiently transfected either by microinjection of plasmid DNA (2 μg/μl in PBS) (Eppendorf Inc. [Fremont, CA] microinjector 5242 and micromanipulator 5171, respectively) into the nucleus of cells growing on gridded coverslips or via electroporation in suspension (Bio-Rad Laboratories [Hercules, CA] GenePulser, 0.25 kV, 500 μF in 400 μl RPMI 1640/25 mM Hepes-KOH, pH 7.3/10 μg DNA) and subsequent plating on No. 1 coverslips. For vital DNA stain, cells were incubated in 100 ng/ml Hoechst 33342 (Molecular Probes, Eugene, OR) in complete medium for 30 min at 37°C, washed three times with PBS, and maintained in fresh complete medium for microscopy.

Electron Microscopy

For conventional electron microscopy, cells transiently expressing LBR–GFP were fixed in culture dishes in 4% paraformaldehyde/0.35% glutaraldehyde in 0.1 M phosphate buffer, pH 7.5, for 1 h at room temperature, postfixed in 1% osmium tetroxide in 0.1 M cacodylate for 1 h, and then block stained with 1% uranyl acetate in 0.1 M sodium acetate overnight on ice. The cells were then dehydrated in a graded ethanol series, removed with propylene oxide from the dishes, and embedded in Araldite resin (CY212; Moreira et al., 1996). Sections 50 nm in thickness were collected on pyoloform-coated nickel grids.

Cryoimmunoelectron microscopy was according to Liou et al. (1996). Briefly, cells expressing LBR–GFP were fixed in the culture dishes by adding one volume of 4% formaldehyde and 0.2% glutaraldehyde to the culture medium for 10 min at room temperature. Fixation was continued for an additional 90 min after diluting the above fixative solution with fresh medium 1:1. After careful removal from the culture dish with a rubber policeman, cells were then rinsed in phosphate buffer/0.15 M glycine and embedded in 10% gelatin. Gelatin blocks were infused with 2.3 M sucrose overnight (rotating at 4°C) and then frozen in liquid nitrogen. Thin cryosections (60 nm) were cut with a cryo ultramicrotome (Reichert Ultracut S/FCS; Leicu, Deerfield, IL) and collected on pyoloform-coated nickel grids. Immunogold labeling on the grids was performed at room temperature using a rabbit polyclonal antibody to GFP (CLONTECH Laboratories) at 1:500 dilution and protein A conjugated with 15-nm gold particles (Biocell, Cardiff, UK). Observation and photography was with an electron microscope (model CM10; Phillips Electronic Instruments, Mahwah, NJ).

Fluorescence Microscopy, Time-Lapse Imaging, and Image Processing

Time lapse imaging was performed using a confocal laser scanning microscope (model LSM 410; Carl Zeiss, Inc., Thornwood, NY) equipped with a triple line Kr/Ar laser, a 100× 1.4 NA Planapochromat oil immersion objective, a 25× 0.8 NA Neofluar immersion corrected objective, and a temperature-controlled stage. Time-lapse sequences were recorded with macros programmed with the Zeiss LSM software package that allow autofocusing on the coverslip surface in reflection mode before taking confocal fluorescence images.

For deconvolved reconstructions, images were captured on a Zeiss Axiophot 100 with identical but motorized 100× objective and a cooled CCD camera (model TFA 2033-K3; Princeton Instruments, Princeton, NJ; Cellscan acquisition unit; Scanalytics, Vienna, VA) followed by processing with exhaustive photon reassignment using the Scanalytics software. Images were background subtracted before quantitation and processing. Fluorescence intensity within regions of interest was quantitated using NIH Image software (Wayne Rasband, RSB, NIH, Bethesda, MD) or the Zeiss LSM software package.

Photobleaching Experiments

FRAP (for review see Edidin, 1994) was performed on a 37°C stage of a Zeiss LSM 410 using the 488-nm line of a 400-mW Kr/Ar laser in conjunction with a 100× objective for optimum resolution or a 25× objective to achieve sufficient depth for bleaching in z. For qualitative experiments shown in Fig. 4, the outlined box was photobleached at full laser power (100% power, 100% transmission) and recovery of fluorescence monitored by scanning the whole cell at low laser power (30% power, 0.3% transmission) in 9-s intervals. The scanning laser intensity did not significantly photobleach the specimen over the time course of the experiment.

For quantitative D measurements listed in Table I, the photobleached strip was 4 μm wide and extended across the cell and through its entire depth. The size and depth of the strip was verified in fixed cells using identical optical parameters. Fluorescence within the strip was measured at low laser power (20% power, 1% transmission) before the bleach (prebleach intensity) and then photobleached with full laser power (100% power, 100% transmission) for 0.97 s (which effectively reduced the fluorescence to background levels in fixed material). Recovery was followed after 2 s with low laser power at 1-s intervals until the intensity had reached a steady plateau. Negligible bleaching occurred while imaging the recovery process at low laser power, as verified in control experiments. The experimental data was fit to the empirical formula given in Eq. 1, which agrees within 5% with the solution of the diffusion equation in one dimension for recovery into an interval of zero intensity:

$$I_{(t)} = I_{(\text{final})} \left(1 - \left(w^2 \left(w^2 + 4\pi D t\right)^{-1}\right)^{1/2}\right) \quad (1)$$

with $I_{(t)}$ = intensity as a function of time, zero of time t was taken as the midpoint of the bleach, i.e., 2.49 s before the first postbleach image; $I_{(\text{final})}$ = final intensity reached after complete recovery; w = strip width, i.e., 4 μm; D = effective one-dimensional diffusion constant. Diffusion constants were calculated by fitting this function to the experimental data

and confirmed by a computer-simulated diffusion starting from a whole-cell prebleach image (see below and Fig. 5, *A* and *B*; Table I).

The above equation assumes one-dimensional recovery, as the membranes are bleached all across their length and entire depth. To assess the effects of geometry, as well as the nonuniform fluorescence density in the ER, we checked *D* calculated from Eq. 1 against a numerical simulation that used the prebleach intensity of the entire cell as input to simulate diffusive recovery into the bleached strip. This required writing computer programs in FORTRAN and C to simulate two-dimensional diffusion in inhomogeneous but isotropic media; the details will be presented elsewhere. Fig. 5, *A* and *B*, shows two sample outputs from these simulations (*circles*). If Eq. 1 is fit primarily to the first 65% recovery (towards the asymptote), the correspondence with the simulation is good. Therefore, for expediency we used the analytic formula in this manner.

On average, the true motion occurs over a longer path along the tubules and cisternae of the ER than observed in a projected image of the cell and interpreted as one-dimensional diffusion. The real diffusion constant is therefore equal or greater than the one extracted from the experiments. For some simple cases, this relation between the effective *D* in Eq. 1 and the true *D* in convoluted membranes is given by Wey et al. (1981). The most important systematic in our study, caused by assuming a single effective *D* to model the entire cell, comes because of the variation in thickness and is at most 30%.

Mobile and immobile fractions were calculated by comparing the intensity ratio in regions of interest inside and outside the bleached area just before the bleach and after recovery. The postbleach intensities were normalized slightly upward to correct for total loss of fluorescence due to the photobleach (typically <10%). The comparison between ER and NE membrane pools in interphase and metaphase in Fig. 5 follows the same FRAP protocol outlined above, except that scanning intensity was increased slightly to compensate for the low intensity levels in ER compared to NE membranes. Scanning intensity was 30% power and 1% transmission and data points were collected every 0.65 s.

Fluorescence loss in photobleaching FLIP experiments were performed on a 37°C stage of a confocal microscope (model LSM 410; Carl Zeiss, Inc.) as described (Cole et al., 1996).

Results

LBR–GFP Localizes and Targets to NE Membranes in the Absence of Cell Division

Previous work has shown that the NH_2 terminus and first transmembrane domain of LBR are sufficient to target heterologous proteins to the inner nuclear membrane (Smith and Blobel, 1993; Soullam and Worman, 1993, 1995). Moreover, all three binding domains for its nucleoplasmic ligands (chromatin, B-type lamins, HP-1) have been mapped to the 208–amino acid NH_2 terminus (Ye and Worman, 1994; Ye et al., 1997). The LBR–GFP fusion protein used in this study contained the first 238 amino acids of LBR, including the nucleoplasmic NH_2 terminus and first transmembrane segment, followed by GFP in the perinuclear space. Thus, the fusion protein should preserve all known functions of the full-length protein.

Localization and targeting of LBR–GFP was investigated in living COS-7 cells after microinjection of an expression plasmid into the nucleus. The distribution of the fusion protein was monitored from the onset of expression using fluorescence imaging with a confocal laser scanning microscope. As shown in Fig. 2 *A* (*3 h postinjection*), LBR–GFP appeared initially in the ER, just outlining the nuclear rim. This pattern colocalized with endogenous ER antigens visualized in fixed cells by indirect immunofluorescence (data not shown). The early appearance of LBR–GFP in the ER is consistent with its synthesis and cotranslational membrane insertion. Over the course of 3–10 h,

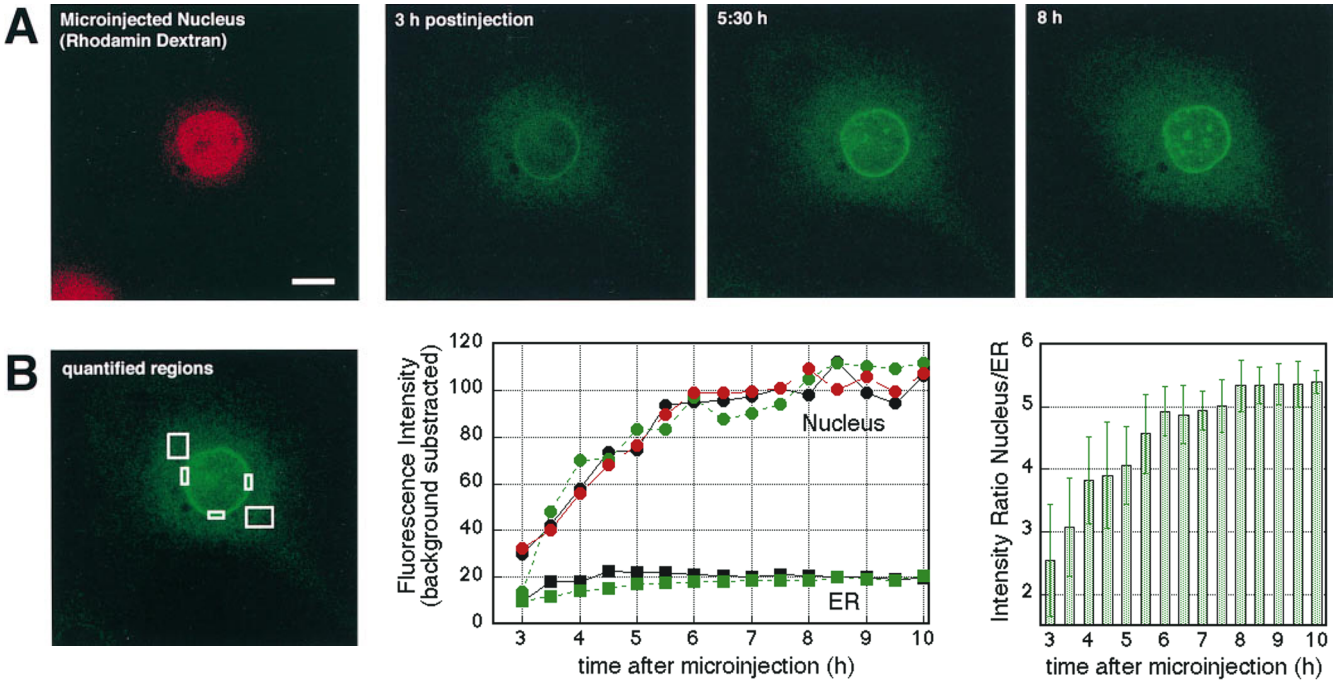

Figure 2. Time course of localization of LBR–GFP to NE membranes. (*A*) Cells were microinjected with an expression plasmid for LBR–GFP along with 70-kD tetramethylrhodamine dextran to mark injected nuclei (*first panel*). Localization of LBR–GFP was followed for 10 h after injection by monitoring the GFP fluorescence every 10 min using a confocal microscope with the pinhole wide open to obtain greatest depth of field. Images shown are after 3, 5.5, and 8 h. (*B*) Representative regions of interest (ROI) in either ER or NE membranes were quantitated in all images taken in *A* (*first panel*). Background subtracted mean fluorescence intensities/area are plotted against time for each of the outlined ROIs in either ER or NE membranes (*line graph*). Ratios of NE fluorescence versus ER fluorescence were calculated from mean values of all ROIs quantitated (*bar graph*). Error bars indicate standard deviation. Data points shown are at 30-min intervals. (The internet URL for quicktime movies is http://dir.nichd.nih.gov/CBMB/pb3labob.htm) Bar, 10 μm.

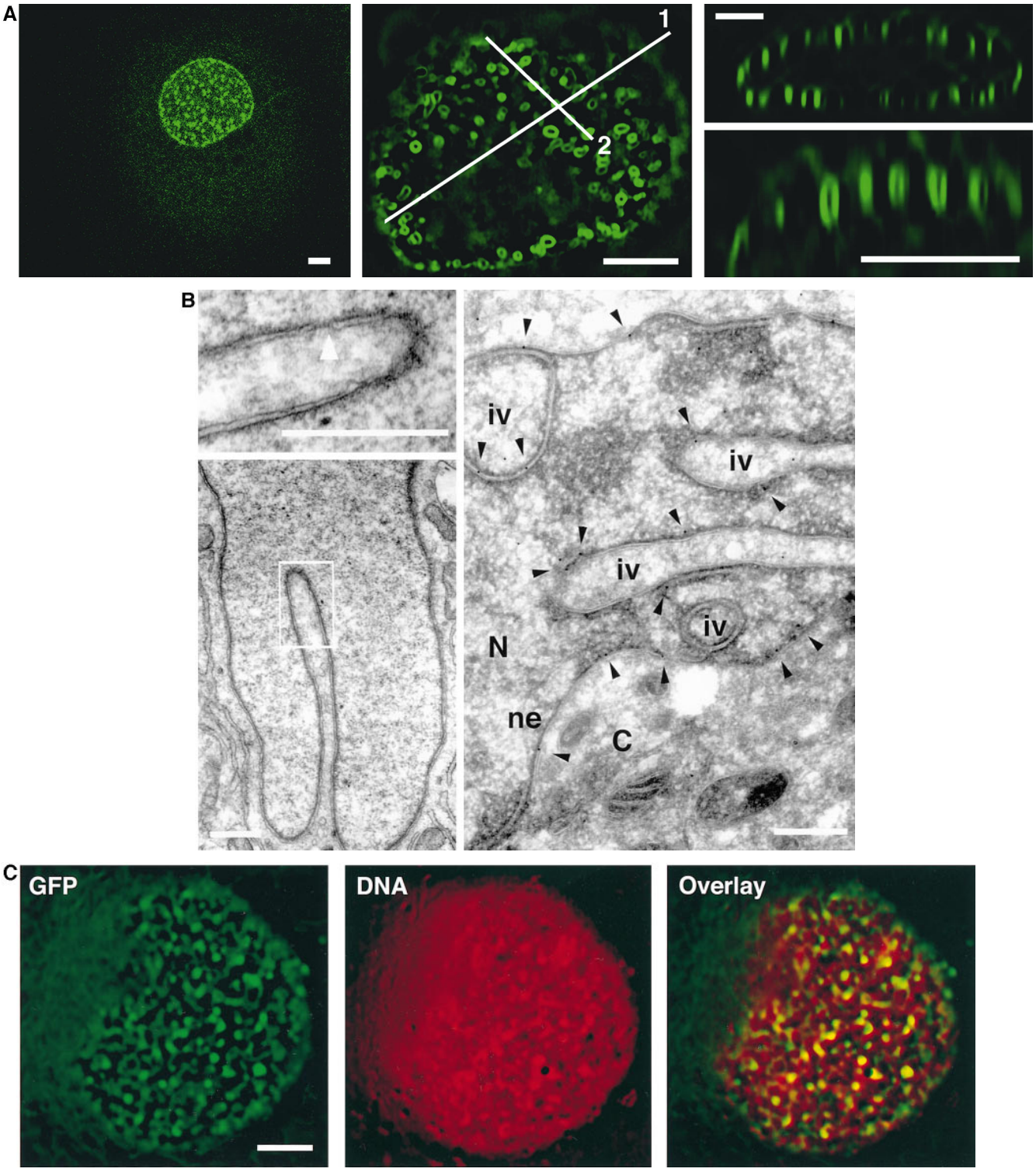

Figure 3. Characterization of NE invaginations labeled by LBR–GFP. (*A*) Deconvoluted serial z-sections of nuclei of living cells expressing LBR–GFP for 48 h were used for a three-dimensional reconstruction of membrane invaginations (see methods). (*Left*) Confocal image of a whole cell showing membrane invaginations in the nucleus. (*Middle*) Deconvolved z-section close to the upper nuclear surface. (*Right*, *top*) Reconstructed projection in z through line 1 indicated in middle panel. (*Right*, *bottom*) Reconstructed projection in z through line 2 from middle panel at higher magnification. (*B*) Electron microscopy images of nuclei from cells transfected with LBR–GFP for 48 h. Left panels show ultrathin sections of Araldite embedded cells. (*Lower left*) Overview of an invagination of the NE double membrane. (*Upper left*) Higher magnification of boxed region with a clearly visible nuclear pore (*arrowhead*). (*Right*) A cryosection from the same cells immunostained with anti-GFP antibody and 15-nm colloidal gold protein A. Note that NE invaginations are specifically labeled with gold particles (*arrowheads*), preferentially between the membranes or on the nucleoplasmic face of the inner nuclear membrane, consistent with the predicted topology of LBR–GFP (Fig. 1). *N*, nucleus, *C*, cytoplasm, *ne*, nuclear envelope, *iv*, invaginations. Note the frequent contacts of electron-dense material with the NE and its invaginations. (*C*) Deconvoluted z-sections of nuclei as in *A*, except that DNA was costained with the vital dye Hoechst 33342. (*Left*) GFP fluorescence in a section close to the lower surface of the nucleus. (*Middle*) Hoechst 33342 fluorescence in pseudocolor red. (*Right*) A merged image, significant colocalization in yellow. Bars: (*A* and *C*) 5 μm; (*B*) 0.5 μm.

LBR–GFP fluorescence accumulated in NE membranes with a constant, low steady-state level in the ER (Fig. 2 *A*). Quantitation of fluorescence per area in different regions in NE and ER membranes showed that the fluorescence in NE membranes reached a plateau at 8 h after injection with a 5.3-fold higher level than in the ER (Fig. 2 *B*). The overall distribution of LBR–GFP at 8 h after injection was indistinguishable from that of endogenous LBR visualized by indirect immunofluorescence (data not shown). Moreover in fixed cells whose plasma membrane had been differentially permeabilized by digitonin, LBR–GFP could be detected only in the ER but not concentrated in the NE with antibodies against the nucleoplasmic domain of LBR, whereas Triton X-100–permeabilized cells showed strong signal in the nuclear rim (data not shown). These results show that LBR–GFP correctly localizes to the nuclear rim, most likely to the inner nuclear membrane, as does full-length native LBR. Furthermore, they demonstrate that targeting to and accumulation of this protein in NE membranes after biosynthesis in ER membranes occurs efficiently in the absence of cell division.

Highly Overexpressed LBR–GFP Accumulates in NE Invaginations That Colocalize with DNA

In addition to the smooth NE labeling observed in cells moderately expressing LBR–GFP, the fusion protein accumulated in defined, regularly spaced structures within NE membranes at high expression levels (Fig. 3 *A*, *left*). To characterize these structures morphologically, a series of images in the z-axis (50 sections/nucleus) were acquired using a digital fluorescence microscope system, followed by deconvolution to reassign out of focus information (Scanalytics, EPR) and three-dimensional reconstruction. Fig. 3 *A* (*middle*) shows a single deconvolved section of nuclear membrane containing LBR–GFP at high magnification and reconstructed projections in the z-plane through lines 1 and 2 (*right*). The LBR–GFP–containing structures were resolved as fingerlike invaginations of the NE that are ~0.5 μm in diameter and reach up to 3 μm into the nucleoplasm, almost always orthogonal from the spherical membrane surface (Fig. 3 *A*, *right*).

Immunogold cryoelectron microscopy using an anti-GFP antibody was performed on LBR–GFP–expressing cells to study the NE invaginations at the ultrastructural level (Fig. 3 *B*). NE invaginations labeled with LBR–GFP gold particles were found to be double membraned and contained nuclear pores (Fig. 3 *B*, *upper left*). Such structures appeared as long deep membrane channels inside the nucleus with cytoplasm extending into them (Fig. 3 *B*, *lower left* and *right*). Electron-dense nucleoplasmic material frequently associated along their rims. LBR–GFP gold labeling was most often observed in regions of nuclear membranes associated with this electron-dense material (Fig. 3 *B*, *right*, *arrowheads*). NE invaginations were more frequently observed in LBR–GFP–expressing than in nonexpressing cells, suggesting their formation was linked to the expression of this protein.

The distribution of DNA-containing chromatin structures in living LBR–GFP–expressing cells was examined by fluorescence microscopy using the vital DNA dye Hoechst 33342. A series of both Hoechst and GFP images were collected in the z-axis and deconvolved in the same manner as for resolving invaginations alone. The distribution of LBR–GFP (Fig. 3 *C*, *GFP*), Hoechst staining (Fig. 3 *C*, *DNA*), and their combined pattern is shown for a single z-section. The yellow structures in the overlay image indicate regions where the labeling patterns of GFP and DNA coincided. Most of these regions of overlap were in the fingerlike invaginations of nuclear membrane where LBR–GFP was enriched and was observed in all z-sections taken. The colocalization was specific and could not be detected in cells expressing LBR–GFP at moderate levels and that did not exhibit NE invaginations (data not shown). This result is consistent with previous in vitro biochemical work demonstrating interactions between LBR and chromatin (Ye and Worman,1994, 1996; Collas et al., 1996; Pyrpasopoulou et al., 1996).

NE and ER Membrane Pools of LBR–GFP Exhibit Different Diffusional Mobilities in Interphase

The finding that LBR–GFP can localize to NE membranes without mitosis and has a small steady-state pool in the ER in interphase (Fig. 4 *A*) led us to investigate whether there are differences in diffusional mobility of the fusion protein in these two compartments. FRAP was used to determine the diffusion constant (*D*) and immobile fraction of LBR–GFP in living cells. The fusion protein was found to be highly mobile in the ER with complete recovery of fluorescence into the bleached area (Fig. 4 *B*, *ER*). Quantitative FRAP experiments determined *D* to be 0.41 ± 0.1 $\mu m^2/s$ in the ER with no significant immobile fraction (Fig. 5 *B*; Table I). The experimental fluorescence recovery exactly followed diffusive kinetics, as demonstrated by the excellent agreement with computer-simulated diffusion assuming a single diffusion constant (Fig. 5 *B*, *circles*). In contrast, LBR–GFP was significantly immobilized within NE membranes. FRAP of the high steady-state levels in the NE membranes showed diffusive recovery only to levels of fluorescence found in ER membranes in the same cells (Fig. 4 *B*, *NE*). Quantitative FRAP could not deter-

Figure 4. Distribution and mobilities of LBR–GFP in interphase and mitotic membranes. (*A*) Confocal section close to the lower cell surface showing steady-state expression of LBR–GFP in an interphase cell. (*Inset*) Boxed region at higher magnification showing LBR–GFP distribution within the ER network. (*B*) Qualitative FRAP experiments in ER and NE membranes in interphase cells expressing LBR–GFP. (*Left*) Photobleach recovery in ER membranes. (*Right*) Photobleach recovery in NE membranes. Note the complete recovery of fluorescence in the ER and the lack of recovery in the NE. (*C*) Thin confocal section through the mitotic apparatus showing the steady-state expression pattern of LBR–GFP in metaphase cells. (*Insets*) Boxed regions at higher magnification showing the tubular membrane network within which LBR–GFP redistributed. Note its resemblance to the interphase ER shown in *A*. (*D*) Qualitative FRAP experiments in mitotic membranes of cells expressing LBR–GFP. (*Left*) Photobleach recovery in prometaphase membranes. (*Right*) Photobleach recovery in telophase membranes. Note the complete recovery of fluorescence in membranes prometaphase but not of telophase. (The internet URL for quicktime movies is http://dir.nichd.nih.gov/CBMB/pb3labob.htm) Bars, 10 μm.

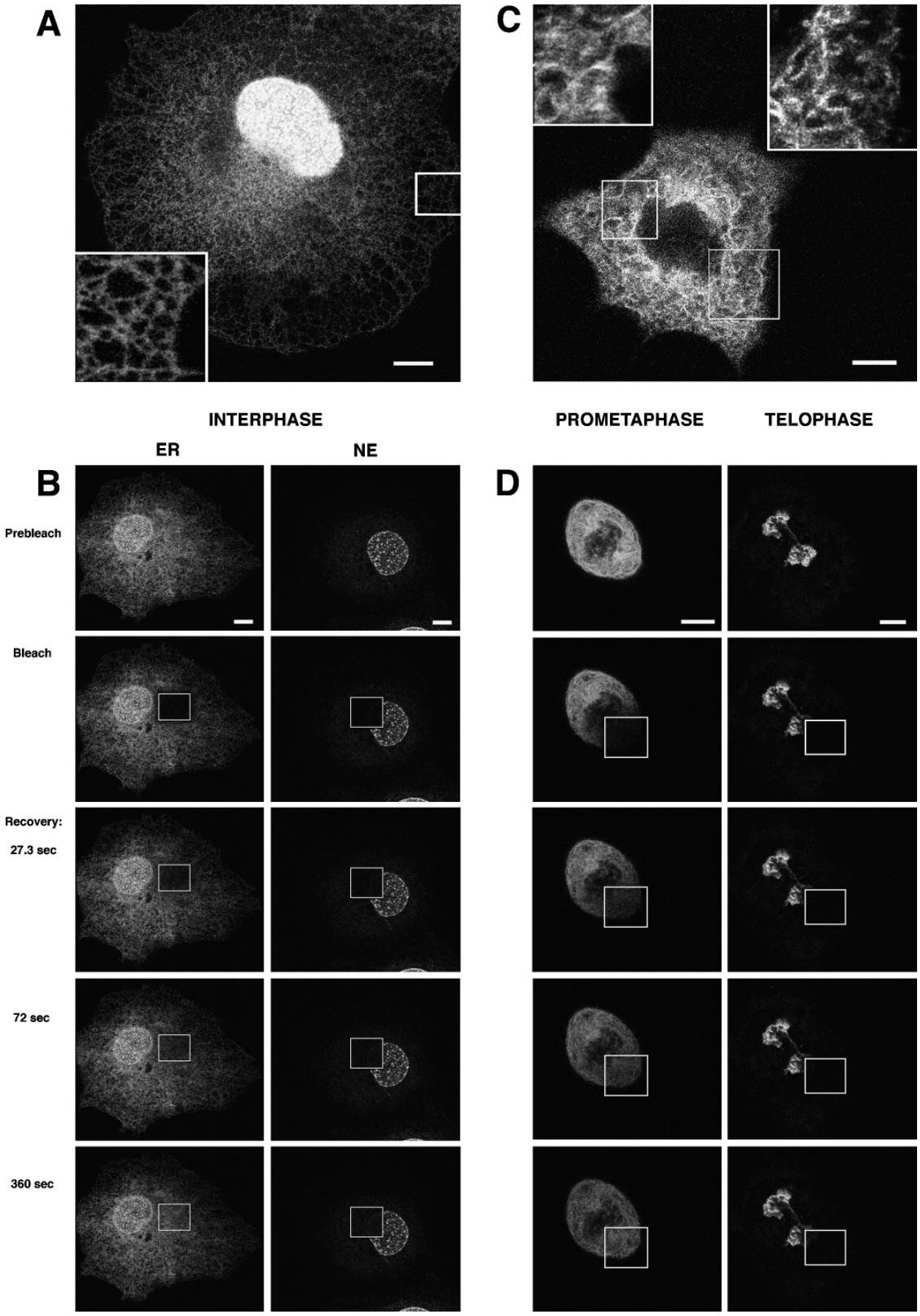
A
C
INTERPHASE
PROMETAPHASE
TELOPHASE
ER
NE
B
D
Prebleach
Bleach
Recovery:
27.3 sec
72 sec
360 sec

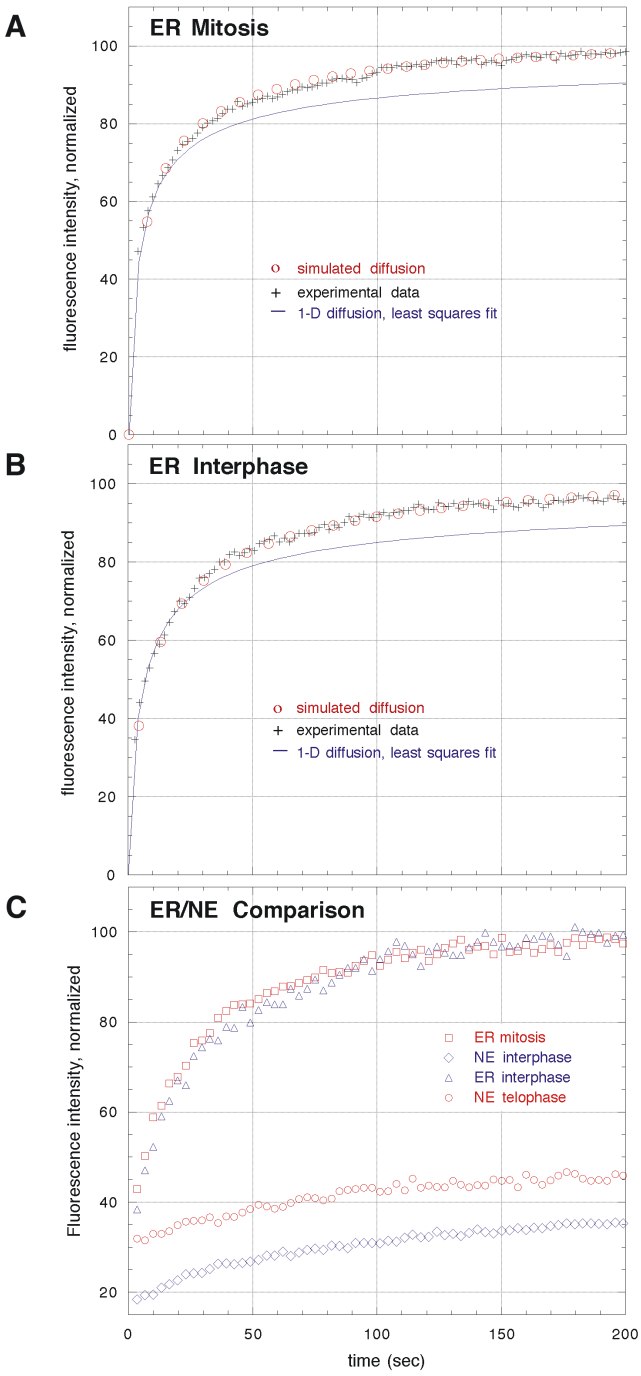

Figure 5. Quantitative FRAP experiments to determine diffusion constants for LBR–GFP. Fluorescence intensities in recovery after photobleaching are plotted versus time. Data points were taken at 1-s intervals until they had reached a steady plateau. (*A* and *B*) FRAP in metaphase membranes (ER mitosis, *A*) or ER membranes in interphase (ER interphase, *B*). Experimental data are marked by crosses, computer-simulated diffusion from a prebleach whole cell image by circles. The simulated intensities overlapped exactly with the experimental data. A least squares fit of Eq. 1 (see Materials and Methods) to the experimental data at early timepoints is shown by a line. The curves displayed kinetics allowing the determination of a single diffusion constant for LBR–GFP in ER membranes in mitotic and interphase cells (see Materials and Methods for details). (*C*) Comparison of FRAP experiments of LBR–GFP in ER and NE membranes in different stages of the cell cycle. ER in interphase (*triangles*), ER in mitosis (*squares*), NE in interphase (*diamonds*), and NE in telophase (*circles*). All experiments were performed under exactly identical conditions for optimal comparison. Note the different kinetics and high immobile fractions in the NE membranes in interphase and telophase. Fluorescence intensity in all panels was normalized to prebleach intensity corrected for total loss of fluorescence because of the high-energy laser bleach to $I_o = 100$ (normalized prebleach intensity). Recovery at $t = 200$ s is therefore a direct measure for the mobile fraction of molecules. See Materials and Methods for experimental details.

Table I. Diffusion Constants (D) and Immobile Fractions of LBR–GFP

Membrane	Cell cycle stage	D	Immobile fraction (%)
		$\mu m^2/s$	
ER	interphase	0.41 ± 0.1*	3.1 ± 3.9*
ER	mitosis	0.38 ± 0.1* ‡	6.4 ± 7.7* ‡
NE	interphase	NA§	>60
NE	telophase	NA§	>55

*Standard deviations are given from a mean of $n \geq 7$ independent determinations.
‡Not significantly different from ER in interphase as determined by t test, $P > 0.5$.
§Not applicable, as immobile fraction rose above 55% and kinetics did not fit a diffusional profile.

mine D in nuclear envelope membranes because the immobile fraction was >60%, and the recovery did not follow diffusive kinetics above ER fluorescence intensity levels (Fig. 5 *C*; Table I). With longer recovery times (e.g., >20 min), fluorescence began to slowly reappear in NE membranes following linear kinetics (data not shown), suggesting slow exchange of the mobile pool in the ER with the immobilized pool in NE membranes. These results demonstrate the same integral membrane protein can exhibit strikingly different diffusional mobilities when localized to different intracellular membrane domains. They also offer a simple explanation for LBR–GFP localization within NE membranes: lateral diffusion from ER to NE membranes, where immobilization mechanisms trap the fusion protein.

During Mitosis LBR–GFP Redistributes into ER Membranes, Where It Is Highly Mobile

Having observed the striking differences in diffusional mobility of LBR–GFP in interphase NE and ER membranes, we asked whether two distinct pools of LBR–GFP are maintained through mitosis after disassembly of the NE in prometaphase. Fig. 4 *D* (*PROMETAPHASE*) shows a FRAP experiment in a typical cell in prometaphase where LBR–GFP was found in membranes distributed throughout the cell. LBR–GFP fluorescence recovered completely within the photobleached box indicating the fusion protein was highly mobile within mitotic membranes. The D (0.38 ± 0.1 $\mu m^2/s$) and immobile fraction (6 ± 7.7%) of LBR–GFP in mitotic membranes was indistinguishable from that of LBR–GFP in interphase ER membranes (Fig. 5 *A*; Table I), regardless of whether the photobleached area was located in the center or the periphery of mitotic cells. As in interphase, the recovery kinetics were precisely diffusive, as confirmed by computer-simulated diffusion with a single diffusion constant (Fig. 5 *A*, *circles*). The high lateral mobility of LBR–GFP remained

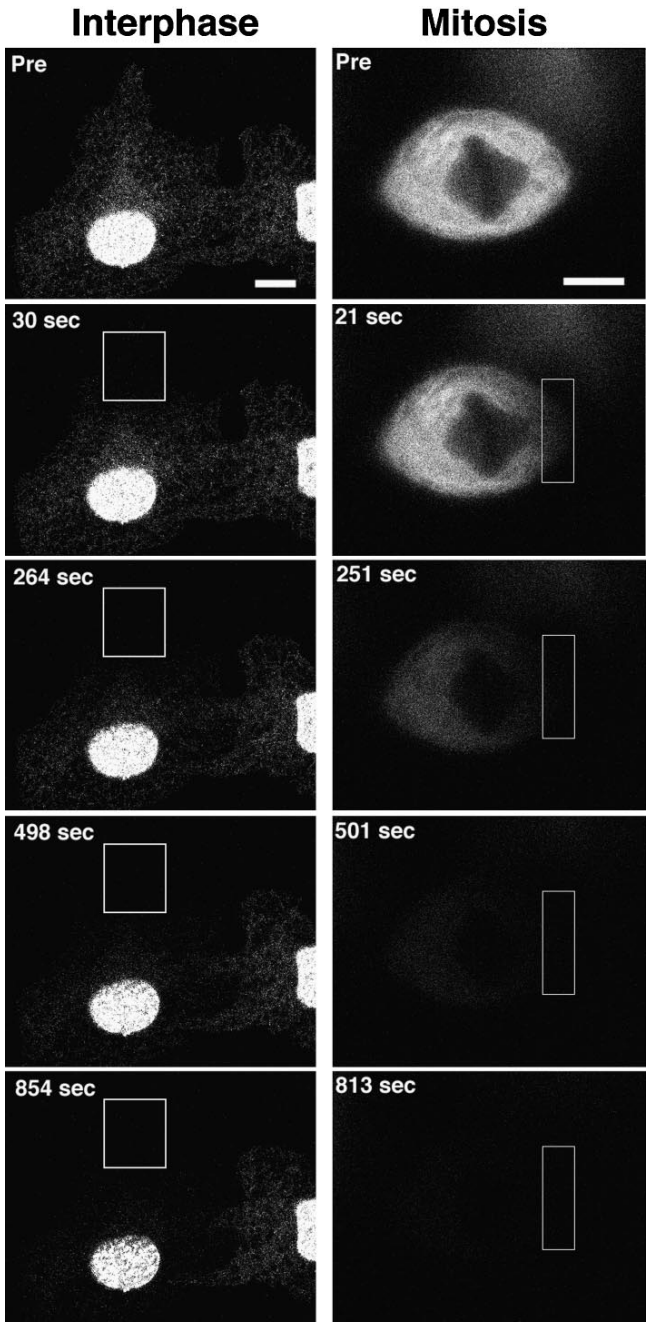

Figure 6. FLIP to probe the continuity of interphase and mitotic membranes containing LBR–GFP. FLIP experiments were performed on interphase membranes (*left*) and metaphase membranes (*right*). Note the complete loss of fluorescence from both interphase ER membranes and mitotic membranes over a similar time course, but not from NE membranes in interphase. ER fluorescence that remained in interphase is from an adjacent cell whose membranes were not connected to those within the photobleached box. Bars, 10 μm.

unchanged up to late anaphase, but upon NE reassembly in late anaphase, FRAP experiments showed that LBR–GFP became immobilized as soon as fluorescent membranes began to accumulate around chromatin (Fig. 4 *D*, *TELOPHASE*). Similar to interphase NE membranes, *D* could no longer be measured in chromatin-associated membranes since the immobile fraction was >55% (Fig. 5 *C*, Table I).

The observation that LBR–GFP in mitotic membranes exhibited a single diffusion constant, which was identical to *D* of LBR–GFP within interphase ER membranes with no significant immobile fraction, raised the possibility that the NE-localized pool of LBR–GFP redistributes into ER membranes upon onset of mitosis rather than into fragmented vesicles. Confocal microscopy confirmed this possibility and revealed LBR–GFP to reside in an extensive tubular membrane network in mitotic cells (Fig. 4 *C*, *insets*) that could be labeled with endogenous ER markers (data not shown) and resembled that of LBR–GFP in interphase ER membranes (Fig. 4, *A* and *C*, *insets*). The tubular membrane network containing LBR–GFP could be observed in all mitotic stages (from prometaphase to telophase). It included cisternal elements that were directly adjacent to the membrane-excluding area of the mitotic apparatus.

The high mobility of LBR–GFP within mitotic membranes and their reticular morphology prompted us to investigate the extent to which these membranes are continuous and whether all regions can contribute to recovery of fluorescence at a bleached site. We used a variation of FRAP, termed FLIP, a technique that uses repetitive photobleaching of a small area and monitors fluorescence loss in the entire cell. FLIP of LBR–GFP was first investigated within interphase cells (Fig. 6, *Interphase*) and revealed a rapid loss of LBR–GFP fluorescence from ER but not NE membranes. This result confirmed previous data (Cole et al., 1996) showing that interphase ER membranes are completely interconnected. That NE membranes were not depleted of LBR–GFP fluorescence during FLIP also confirmed the immobilization of the fusion protein within NE membranes since interphase ER and NE membranes are interconnected.

FLIP experiments were next performed in mitotic cells (Fig. 6, *Mitosis*) and revealed the complete loss of LBR–GFP fluorescence associated with mitotic membranes outside the rectangular box in <500 s upon repetitive photobleaching inside the box. This result implies that mitotic membranes containing LBR–GFP are extensively interconnected, with the fusion protein diffusing freely and rapidly from one region to another. Since ER membranes within mitotic cells have been previously shown to remain interconnected, as in interphase cells (Porter and Machado, 1960; Zatespina et al., 1977; Waterman-Storer et al., 1993), these results are consistent with redistribution of LBR–GFP into ER membranes during mitosis rather than into isolated NE membrane fragments or vesicles.

Kinetics and Intermediates of Nuclear Membrane Reassembly after Mitosis

To resolve the structures that mediate NE membrane reassembly and to describe the dynamics of this process in vivo, we used high-resolution time-lapse confocal microscopy. Living cells expressing LBR–GFP were imaged from anaphase through cytokinesis by taking confocal sections through the cell every 15 s (Fig. 7 *A*). The sequences revealed a nuclear membrane reassembly process involving redistribution of LBR–GFP from diffusely distributed reticular membranes to membranes tightly associated with chromatin that expanded into spherical NE (Fig. 7 *A*). The initial reassembly of the nuclear membranes around two

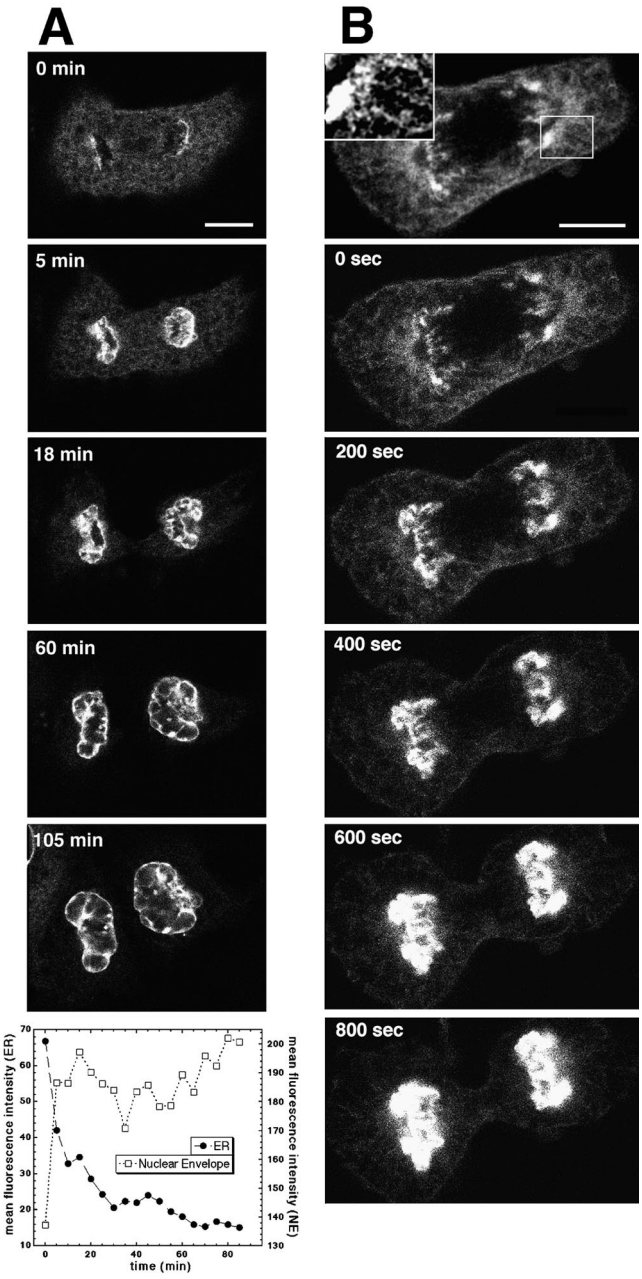

Figure 7. NE membrane reassembly in vivo. (*A*) Time-lapse sequence from late anaphase to cytokinesis covering complete NE reformation. Confocal images were taken every 15 s. Graph shows quantitation of representative ROIs in ER and NE membranes for the time-lapse sequence shown. Note the correlation of loss of fluorescence from the ER with the sudden concentration of fluorescent material in the NE. (*B*) Time-lapse sequence of the first 13 min of NE membrane reassembly in late anaphase. Thin confocal sections were taken every 8 s through the reforming nuclei to resolve the ER reticulum. (The internet URL for quicktime movies is http://dir.nichd.nih.gov/CBMB/pb3labob.htm) Bar, 10 μm.

pronuclei was a highly dynamic process. Typically, only 3–5 min elapsed between the first detectable fluorescence accumulation in peripheral caps on the chromosomal material (Fig. 7 *A*, *first panel*) and a complete enclosure and sealing of the chromatin by this membrane (Fig. 7 *A*, *second panel*). Nuclear membrane closure was followed by a slower growth and expansion of these membranes. As the NE expanded, extensive invaginations and infoldings of membranes enriched in LBR–GFP were observed (Fig. 7 *A*, *last two panels*).

Quantification of regions in the ER and on growing NE membranes revealed a rapid initial concentration of LBR–GFP fluorescence in NE membranes that correlated exactly with a drop of fluorescence signal from the ER (Fig. 7 *A*, *graph*). After this initial accumulation in nuclear membranes, the fluorescence intensity per area in these membranes remained relatively constant. ER membranes, however, kept losing fluorescence because of continual expansion of NE membrane surface area with recruitment of LBR–GFP molecules.

To gain further insight into the structures mediating nuclear membrane reassembly, we acquired high-resolution images at 8-s time intervals during the first 10 min after concentration of LBR–GFP around chromatin was detected (Fig. 7 *B*, *second panel*). Thin confocal sections through the center of the assembling NE membranes revealed tubular elements of the ER directly connected to concentrations of immobilized LBR–GFP in membranes wrapping around the chromatin (Fig. 7 *B*, *inset*). Numerous tubular membrane connections between this chromatin-associated membrane sheet and the rest of the ER appeared to be a constant feature of the reassembly process (Fig. 7 *B*, sequence). These results demonstrate that formation and enclosure of reassembling nuclear membranes is a rapid process involving membranes of a continuous ER/nuclear membrane system.

Discussion

Lamin B Receptor Targeting and Mobility in Interphase

Our results show that a LBR–GFP fusion protein is synthesized in the ER membrane and then targeted to and localized in the inner nuclear membrane without requiring cell division. FRAP experiments revealed LBR–GFP to diffuse freely in ER membranes (D = 0.41 $\mu m^2/s$) but to be immobilized within NE membranes (immobile fraction >60%). As discussed below, these properties suggest a targeting mechanism of LBR–GFP to the inner nuclear membrane that involves lateral diffusion through ER membranes into the outer nuclear membrane, movement around the nuclear pore complex through the pore membrane into the inner nuclear membrane, and subsequent immobilization by known interactions with chromatin or the lamina.

Rapid and free diffusion of LBR–GFP in ER membranes was demonstrated by its complete recovery in FRAP experiments with a D value of 0.41 $\mu m^2/s$, comparable to other ER-localized membrane protein–GFP fusions, including the human KDEL receptor ELP1, which has a D of 0.43 $\mu m^2/s$ (Hsu et al., 1992; Cole et al., 1996). Free diffusion of LBR–GFP throughout the entire interconnected ER membrane system, which is continuous with the outer nuclear membrane, was shown by FLIP experiments where repeated photobleaching of a small portion of the ER resulted in complete loss of ER-associated LBR–GFP fluorescence. Accessibility of the outer nuclear membrane

for LBR–GFP from the ER was indicated by FRAP experiments on NE membranes, where fluorescence in the nuclear rim recovered only to levels present in the ER with diffusional kinetics.

The extensive immobilization of LBR–GFP observed in NE membranes is most likely to occur in the inner nuclear membrane through known binding interactions with chromatin or the lamina (Ye and Worman, 1994, 1996; Collas et al., 1996; Pyrpasopoulou et al., 1996; Ye et al., 1997), which are not accessible from the outer nuclear membrane. Such interactions would serve as an efficient retention mechanism to prevent diffusion back into the outer nuclear membrane and has been suggested previously in heterokaryon experiments for a different inner nuclear membrane protein (Powell and Burke, 1990). Support for a LBR–GFP/nucleoplasmic ligand interaction comes from our finding that NE invaginations containing LBR–GFP colocalized with chromatin structures inside the nucleus. Moreover, the large immobile fraction of LBR–GFP in NE membrane revealed from FRAP experiments indicated a tight binding to a fixed structural component of the nucleus rather than retention merely by assembly into multimeric complexes (Simos and Georgatos, 1992; Smith and Blobel, 1993), which would be expected to have a low diffusion rate but still some lateral mobility. GFP-labeled nuclear pore complex components, for example, have been shown to diffuse slowly within NE membranes (Belgareh and Doyé, 1997; Bucci and Wente, 1997).

The above results provide the first measurements of the diffusional mobility of a defined inner nuclear membrane protein and suggest an "immobilization trap" mechanism for targeting and retention of integral membrane proteins in the inner nuclear membrane. Previous data addressing the mobility of proteins in NE membranes have been obtained in vitro using isolated nuclei chemically modified with citraconic acid to expose the inner nuclear membrane. In such studies, D for proteins bound by the fluorescently labeled lectin wheat germ agglutinin was determined to be 0.039 $\mu m^2/s$ in the outer membrane (suggesting slow diffusion) and not detectable in the inner membrane (Schindler et al., 1985). Results from our FRAP studies suggest that LBR–GFP is highly mobile within ER membranes as well as in the outer nuclear membrane (which are continuous with each other) but is completely immobilized within the inner nuclear membrane. The small pool of LBR–GFP in NE membranes, which did recover above ER levels of fluorescence after photobleaching, showed slow nondiffusive linear kinetics. This could reflect a restricted diffusion of LBR–GFP from ER/outer nuclear membrane through the pore membrane to the inner nuclear membrane since the lateral membrane channels of nuclear pore complexes are likely to impose a sterical constraint on diffusion (Hinshaw et al., 1992; Akey, 1995; Soullam and Worman, 1995).

NE Invaginations

NE invaginations enriched in LBR–GFP were only observed in large numbers in cells overexpressing the fusion protein at high levels. We could not detect obvious abnormalities (such as timing or number of cell divisions) other than the increased number of invaginations in such cells. The fingerlike structures measured 0.5 μm in diameter, were orthogonal to the NE membrane, and reached up to 3 μm into the nucleoplasm where they colocalized with DNA/chromatin. Cryoimmunoelectron microscopy showed these to consist of a cytoplasmic invagination bounded by a double membrane, which contained nuclear pores and could be specifically decorated by anti-GFP antibodies. Nuclear membrane invaginations of this type have been reported in EM studies (Bourgeois et al., 1979; Hochstrasser and Sedat, 1987; Parke and de Boni, 1992) and appear to be a permanent feature of interphase nuclei in mammalian cells. Recently, Fricker et al. (1997) have characterized these structures, showing that they penetrate deep into the nucleus as membrane channels and vary in number and morphology in different cell types.

The number of NE invaginations was increased by overexpression of LBR–GFP. That these invaginations were directed into the nucleoplasm instead of outward to the cytosol, however, argues against them merely providing additional surface area to accommodate excess membrane protein. Their colocalization with DNA markers instead favors the possibility that they play a role in the spatial organization of NE/chromatin interface through interactions with the nucleoplasmic domain of LBR. This type of organization appeared to be dynamic since NE invaginations accumulated in number during overexpression of LBR–GFP, and their formation did not require cell division.

Redistribution and Diffusional Mobility of LBR–GFP in Mitosis

High-resolution confocal imaging of mitotic cells revealed LBR–GFP to redistribute into the ER membrane network, colocalizing with endogenous ER markers. These membranes exhibited an extensive tubular morphology in all mitotic stages, resembling interphase ER. They were completely interconnected, as demonstrated by FLIP experiments using LBR–GFP. Within mitotic ER membranes, LBR–GFP exhibited the same high diffusional mobility as in interphase ER membranes ($D = 0.38 \pm 0.1$ $\mu m^2/s$, no significant immobile fraction). The fusion protein redistributed from NE membranes into ER membranes in prometaphase and remained in this membrane network until the onset of NE reassembly in late anaphase.

The finding of an intact ER membrane system in mitosis that contained an inner nuclear membrane protein, such as LBR–GFP, was surprising since it contrasted with the generally accepted view that NE membranes vesiculate completely during mitosis (Robbins and Gonatas, 1964; Wasserman and Smith, 1978; Zeligs and Wollman, 1979; Marshall and Wilson, 1997). This view has been given greatest support from biochemical studies using mitotic NE precursor membranes derived from membrane homogenates of mitotic cells or *Xenopus* oocytes (Newport and Dunphy, 1992; Chaudhary and Courvalin, 1993; Marshall and Wilson, 1997). During preparation of such homogenates, however, membranes easily become vesiculated and fragmented, in contrast to undisturbed membranes of intact living cells. Refinements of these studies have even revealed two or more distinct vesicle populations enriched in different integral NE membrane proteins (Vigers and Lohka, 1991; Chaudhary and Courvalin, 1993; Buendia

and Courvalin, 1997). This is not contradictory to an ER localization of these molecules before homogenization, however, since particular proteins may have distinct affinities for different ER microdomains and thus become enriched in vesicles of different composition upon homogenization. Our results do not dispute that vesicles can form NE structures in vitro. They strongly suggest, however, that this does not occur in living mammalian cells.

We could not visualize vesicle intermediates at any stage of mitosis during imaging of LBR–GFP redistribution in living cells, despite the fact that the GFP variant used allows us to detect structures as small as caveoli (not shown; see also Niswender et al., 1995). Furthermore, vesicles and membrane fragments are unlikely to diffuse sufficiently fast throughout the entire cell to result in complete loss of fluorescence over the time course of the FLIP experiments. For example, FLIP experiments on discontinuous membrane systems such as fluorescently labeled endosomes and lysosomes revealed these to have a dramatically slower loss of fluorescence than GFP-tagged membrane proteins in mitotic ER (Zaal, K.J.M., personal communication).

The accuracy with which computer simulations based on a single diffusion constant quantitatively fit the experimental photobleach recovery in mitosis provides an additional powerful argument against LBR–GFP–containing vesicles. To give rise to the measured diffusive kinetics, hypothetical vesicles would have to be of uniform size (within 26% of the same radius, based on the standard deviation of our *D* measurements, as *D* is inversely proportional to the radius) and would coincidentally diffuse at exactly the same rate as LBR–GFP in interphase ER membranes. Vesicles with a diffusion rate different than LBR–GFP in mitotic ER could only contain $<7\%$ of the overall fluorescence intensity if they diffuse slower than LBR–GFP (A higher percentage would be detected as a significant immobile fraction in FRAP experiments.) or $<10\%$ if they diffuse faster. (Twofold or more; a higher intensity percentage would lead to serious misalignment of the computer-simulated diffusion with the photobleaching recovery curves.) The fact that our *D* measurements were uniform throughout the mitotic cell (center versus periphery) argues against a spatially specialized pool of vesicles.

Our observation that ER membranes remain interconnected during mitosis is consistent with several studies that have shown the ER to stay as an intact reticulum during division in many cell types. These include onion root tip (Porter and Machado, 1960), developing sea urchin embryo (Terasaki, M., personal communication), porcine kidney (Zatespina et al., 1977), T cells (Peters, P., personal communication), chicken erythroblasts (Stick et al., 1988), and highly adherent epithelial cells such as PtK_2 (Waterman-Storer et al., 1993; Ioshii et al., 1995). Although ER vesiculation during mitosis has been proposed, even widely cited references (Robbins and Gonatas, 1964; Zeligs and Wollman, 1979) contain evidence for persistent cisternal ER elements in several cell types.

Dynamics of NE Membrane Reassembly from ER Elements

Beginning in late anaphase, the highly mobile pool of LBR–GFP within interconnected tubular ER membranes extending throughout the cytoplasm redistributed into membranes tightly folded around chromatin. This process started in peripheral caps on the chromatin, areas that are exposed to ER membranes first as the spindle apparatus breaks down. Within 2 min, the concentration of LBR–GFP in these membranes grew immensely, fed by ER tubules that were directly connected to them. Simultaneously, an equal amount of fluorescence was lost from the ER without notable concentration gradients between central and peripheral ER. This demonstrated that the reassembly process is not limited by diffusion of LBR–GFP within ER membranes despite its high speed. FRAP experiments revealed LBR–GFP to be extensively immobilized within chromatin-associated membranes in early telophase, comparable to interphase NE membranes. As these intensely labeled membranes accumulated more surface area, they wrapped around the chromatin forming an enclosed nuclear membrane envelope. The wrapping mechanism was extremely rapid and occurred before significant chromatin decondensation in late anaphase. Thus, it is unlikely to depend on preassembly of the nuclear lamina, which is in good agreement with data reported previously in fixed cells (Chaudhary and Courvalin, 1993).

After wrapping and closure around condensed chromatin, the newly formed nuclear membrane expanded into a spherical structure over the course of 30–80 min from telophase to cytokinesis. This growth process coincided with chromatin decondensation and presumably involved nuclear import of cytoplasmic components, such as soluble lamins, and their subsequent polymerization. During their expansion, the nuclear membranes exhibited extensive invaginations and infoldings. LBR–GFP was enriched within these membrane infoldings, raising the possibility that its heterochromatin-binding properties could have an important role in spatially organizing chromatin within the nucleus before entry into G1.

NE Membrane Disassembly and Reformation: A Model

Our biophysical and morphological observations on LBR–GFP localization and dynamics are most plausibly explained by the following model for NE membrane disassembly and reformation (Fig. 8). In interphase, newly synthesized integral membrane proteins of the inner nuclear membrane, such as LBR, move from their site of membrane insertion in the ER into the inner nuclear membrane by lateral diffusion through a continuous proteolipid bilayer. Once in the inner surface of the NE, they become immobilized by binding to nucleoplasmic ligands. During prometaphase, these proteins would lose their binding affinity to nucleoplasmic ligands through phosphorylation by mitotic kinases of receptor and/or ligand and diffuse into the directly connected membrane system of the ER, where they remain highly mobile throughout mitosis. Disassembly of nuclear pore complexes could occur either concurrently or soon thereafter, resulting in NE membranes as a whole being rapidly absorbed into the larger surface area of the ER, leaving no envelope structure remaining.

NE reassembly in late anaphase would be mediated by the reverse process. The phosphorylation state of LBR and other inner nuclear membrane receptors and their ligands on the chromatin would switch back, mediated by

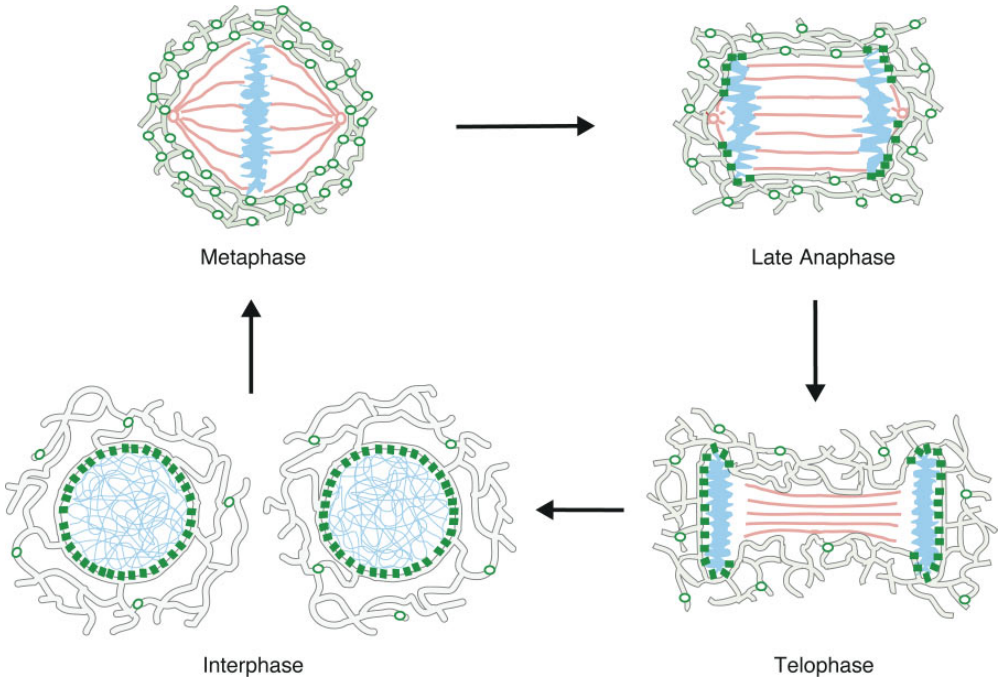

Figure 8. Model of nuclear envelope reassembly. In interphase (*bottom left*), newly synthesized integral inner nuclear membrane proteins such as LBR (*green ovals*) move by lateral diffusion from the ER (*gray outlined network*) to the inner nuclear membrane, where they are retained and immobilized (*green squares*) by binding to nucleoplasmic ligands (chromatin, *blue*). Early in mitosis, these binding interactions are disrupted, leading to equilibration of the mobilized LBR molecules within the ER/NE system. In metaphase (*top left*) the NE is completely disassembled and LBR diffuses freely within an interconnected ER network that surrounds the spindle apparatus (*red*) and the condensed chromatin. Binding sites for LBR are available again in late anaphase (*top right*), immobilizing the receptor at contact sites between ER and chromatin. Towards telophase (*bottom right*), more binding sites become exposed as the spindle retracts, trapping more LBR molecules and forcing ER membranes to wrap around the chromatin. This progressive immobilization and wrapping leads to a rapid and efficient enclosure of nuclear material by ER elements highly enriched in LBR, which form the new NE. From telophase to early interphase, the NE expands slowly into a sphere surrounding the decondensed chromatin. The majority of LBR has localized to the inner nuclear membrane and remains there throughout interphase (*bottom left*).

a change in kinase/phosphatase equilibrium. This change would allow rebinding between condensed chromatin structures and LBR in ER elements in close proximity, immobilizing the receptor. As additional LBR molecules diffused into these membrane domains, they also would bind chromatin and be retained. Through such a process, chromatin would progressively be wrapped by an LBR-containing membrane sheet and be quickly sealed off from the cytoplasm.

NE reassembly by coalescence of ER elements as opposed to vesicles has been proposed from ultrastructural studies dating back to 1960 (Porter and Machado, 1960; Robbins and Gonatas, 1964; Zatespina et al., 1977), some of which show ribosomes on the nucleoplasmic surface of NE precursor structures (Zatespina et al., 1977). Our results following NE reassembly in vivo provide strong evidence in favor of this view. They suggest that the same basic processes at work during interphase that localize inner nuclear membrane proteins from the ER can explain mitotic redistribution of these molecules. Such processes involve cell cycle–dependent changes in adhesion of NE proteins to nucleoplasmic ligands, which lead to changes in their retention and distribution within an interconnected ER/NE membrane system.

We thank Jean-Claude Courvalin (Institute Jacques Monod–CNRS, Paris, France) and Mark Terasaki (University of Connecticut, Farmington, CT) for insightful discussions regarding this work. We would also like to thank Ron Maimon, (Cornell University, Ithaca, NY) for help with the computer simulation software and Richard Klausner, Juan Bonafacino, Koret Hirschberg, Sarah Nehls, Kristien Zaal (all at National Institute of Child Health and Human Development, NIH, Bethesda, MD) and Silke Schumacher (National Institute of Diabetes and Digestive and Kidney Disorders, NIH, Bethesda, MD) for critical reading of the manuscript.

J. Ellenberg was supported by a predoctoral fellowship of the Boehringer Ingelheim Fonds, Germany. H.J. Worman is an Irma T. Hirschl Scholar and supported by grants from the National Institutes of Health (RO1-CA66974) and the American Cancer Society (RPG-94-006-03-CB).

Received for publication 27 May 1997 and in revised form 27 June 1997.

Note Added in Proof. Recent data of Yang et al. (1997. *J. Cell Biol.* 137: 1199–1210) in fixed cells have provided evidence for colocalization of ER markers with integral membrane proteins of the nuclear envelope during mitosis.

References

Akey, C.W. 1995. Structural plasticity of the nuclear pore complex. *J. Mol. Biol.* 248:273–293.

Belgareh, N., and V. Doyé. 1997. Dynamics of nuclear pore distribution in nucleoporin mutant yeast cells. *J. Cell Biol.* 136:747–759.

Bergman, J., and J. Singer. 1983. Immunoelectron microscopic studies of the intracellular transport of the membrane glycoprotein (G) of vesicular stomatitis virus in infected Chinese hamster ovary cells. *J. Cell Biol.* 97:1777–1787.

Bione, S., E. Maestrini, S. Rivella, M. Mancini, S. Regis, G. Romeao, and D. Toniolo. 1994. Identification of a novel X-linked gene responsible for Emery-Dreifuss muscular dystrophy. *Nature Genet.* 8:323–329.

Bourgeois, C.A., D. Hemon, and M. Bouteille. 1979. Structural relationship between the nucleolus and the nuclear envelope. *J. Ultrastruct. Res.* 68:328–340.

Bucci, M., and S. Wente. 1997. In vivo dynamics of the nuclear pore complexes in yeast. *J. Cell Biol.* 136:1185–1200.

Buendia, B., and J.-C. Courvalin. 1997. Domain-specific disassembly and reassembly of nuclear membranes during mitosis. *Exp. Cell Res.* 230:133–144.

Chalfie, M., Y. Tu, G. Euskirchen, W.W. Ward, and D.C. Prasher. 1994. Green fluorescent protein as a marker for gene expression. *Science (Wash. DC).* 263:802–805.

Chaudhary, N., and J.-C. Courvalin. 1993. Stepwise reassembly of the nuclear envelope at the end of mitosis. *J. Cell Biol.* 122:295–306.

Cole, N.B., C.L. Smith, N. Sciaky, M. Terasaki, M. Edidin, and J. Lippincott-

Schwartz. 1996. Diffusional mobility of Golgi proteins in membranes of living cells. *Science (Wash. DC).* 273:797–801.
Collas, P., J.-C. Courvalin, and D. Poccia. 1996. Targeting of membranes to sea urchin sperm chromatin is mediated by a lamin B receptor-like integral membrane protein. *J. Cell Biol.* 135:1715–1725.
Courvalin, J.-C., N. Segil, G. Blobel, and H.J. Worman. 1992. The lamin B receptor of the inner nuclear membrane undergoes mitosis-specific phosphorylation and is a substrate for $p34^{cdc2}$-type protein kinase. *J. Biol. Chem.* 267:19035–19038.
Edidin, M. 1994. Fluorescence photobleaching and recovery, FPR, in the analysis of membrane structure and dynamics. *In* Mobility and Proximity in Biological Membranes. S. Damjanocich, M. Edidin, and J. Szollosi, editors. CRC Press, Inc., Boca Raton, FL. 109–135.
Favreau, C., H.J. Worman, R.W. Wozniak, T. Frappier, and J.-C. Courvalin. 1996. Cell cycle-dependent phosphorylation of nucleoporins and nuclear pore membrane protein gp210. *Biochemistry.* 35:8035–8044.
Foisner, R., and L. Gerace. 1993. Integral membrane proteins of the nuclear envelope interact with lamins and chromosomes, and binding is modulated by mitotic phosphorylation. *Cell.* 73:1267–1279.
Fricker, M., M. Hollinshead, N. White, and D. Vaux. 1997. Interphase nuclei of many mammalian cell types contain deep, dynamic, tubular membrane-bound invaginations of the nuclear envelope. *J. Cell Biol.* 136:531–544.
Furukawa, K., N. Panté, U. Aebi, and L. Gerace. 1995. Cloning of a cDNA for lamina-associated polypeptide 2 (LAP2) and identification of regions that specify targeting to the nuclear envelope. *EMBO (Eur. Mol. Biol. Organ.) J.* 14:1626–1636.
Gerace, L., and G. Blobel. 1980. The nuclear envelope lamina is reversibly depolymerized during mitosis. *Cell.* 19:277–287.
Gerace, L., and B. Burke. 1988. Functional organization of the nuclear envelope. *Ann. Rev. Cell Biol.* 4:335–374.
Hinshaw, J.E., B.O. Carragher, and R.A. Milligan. 1992. Structure and design of the nuclear pore complex. *Cell.* 69:1133–1141.
Hochstrasser, M., and J.W. Sedat. 1987. Three-dimensional organization of *Drosophila melanogaster* interphase nuclei. II. Chromosome spatial organization and gene regulation. *J. Cell Biol.* 104:1471–1483.
Hsu, V.W., N. Shah, and R.D. Klausner. 1992. A brefeldin A-like phenotype is induced by the overexpression of a human ERD-2 like protein, ELP-1. *Cell.* 69:625–635.
Ioshii, S.O., T. Yoshida, K. Imanaka-Yoshida, and K. Izutsu. 1995. Distribution of a Ca^{2+} storing site in PtK_2 cells during interphase and mitosis. An immunocytochemical study using an antibody against calreticulin. *Eur. J. Cell Biol.* 66:82–93.
Liou, W., H.J. Geuze, and J.W. Slot. 1996. Improving structural integrity of cryosections for immunogold labeling. *Histochem. Cell Biol.* 106:41–58.
Lohka, M.J. 1988. The reconstitution of nuclear envelopes in cell-free extracts. *Cell Biol. Int. Rep.* 12:833–848.
Macauley, C., E. Meier, and D.J. Forbes. 1995. Differential mitotic phosphorylation of the nuclear pore complex. *J. Biol. Chem.* 270:254–262.
Marshall, I.C.B., and K.L. Wilson. 1997. Nuclear envelope assembly after mitosis. *Trends Cell Biol.* 7:69–74.
Martin, L., C. Crimaudo, and L. Gerace. 1995. cDNA cloning and characterization of lamina-associated polypeptide 1C (LAP1C), an integral protein of the inner nuclear membrane. *J. Cell Biol.* 270:8822–8828.
Moreira, J.E., T.S. Reese, and B. Kachar. 1996. Freeze-substitution as a preparative technique for immunoelectronmicroscopy: evaluation by atomic force microscopy. *Microsc. Res. Tech.* 33:251–261.
Nagano, A., R. Koga, M. Ogawa, Y. Kurano, J. Kawada, R. Okado, Y.K. Huyashi, R. Tsu Kakaro, and K. Arahata. 1996. Emerin deficiency at the nuclear membrane in patients with Emery-Dreifuss muscular dystrophy. *Nature Genet.* 12:254–259.
Newport, J.W., and W. Dunphy. 1992. Characterization of the membrane binding and fusion events during nuclear envelope reassembly using purified components. *J. Cell Biol.* 116:295–306.
Nikolakaki, E., J. Meier, G. Simos, and S.D. Gergatos. 1997. Mitotic phosphorylation of the lamin B receptor by a serine/arginine kinase and $p34^{cdc2}$. *J. Biol. Chem.* 272:6208–6213.
Niswender, K.D., S.M. Blackman, L. Rohde, M.A. Magnuson, and D.W. Piston. 1995. Quantitative imaging of green fluorescent protein in cultured cells: comparison of microscopic techniques, use in fusion proteins and detection limits. *J. Microsc.* 180:109–116.
Parke, P.C., and U. de Boni. 1992. Nuclear membrane modifications in polytene nuclei of *Drosophila melanogaster*: serial reconstruction and cytochemistry. *Anat. Rec.* 234:15–26.
Pfaller, R., C. Smythe, and J.W. Newport. 1991. Assembly/disassembly of the nuclear envelope membrane: cell cycle-dependent binding of nuclear membrane vesicles to chromatin in vitro. *Cell.* 65:209–217.
Porter, K.R., and R.D. Machado. 1960. Studies on the endoplasmic reticulum. IV. Its form and distribution during mitosis in cells of onion root tip. *J. Biophys. Biochem. Cytol.* 7:167–180 (Pl. 81–96).
Powell, L., and B. Burke. 1990. Internuclear exchange of an inner nuclear membrane protein (p55) in heterokaryons: in vivo evidence for the interaction of p55 with the nuclear lamina. *J. Cell Biol.* 111:2225–2234.
Pyrpasopoulou, A., J. Meier , C. Maison, G. Simos, and S. Georgatos. 1996. The lamin B receptor (LBR) provides essential docking sites at the nuclear envelope. *EMBO (Eur. Mol. Biol. Organ.) J.* 15:7108–7119.
Robbins, E., and N.K. Gonatas. 1964. The ultrastructure of a mammalian cell during the mitotic cell cycle. *J. Cell Biol.* 21:429–463.
Rothman, J.E., and F.T. Wieland. 1996. Protein sorting by transport vesicles. *Science (Wash. DC).* 272:227–234.
Sambrook, J., E.F. Fritsch, and T. Maniatis. 1989. Molecular Cloning: A Laboratory Manual. Cold Spring Harbor Laboratory Press, Cold Spring Harbor, NY.
Schindler, M., J.F. Holland, and M. Hogan. 1985. Lateral diffusion in nuclear membranes. *J. Cell Biol.* 100:1408–1414.
Simos, G., and S.D. Georgatos. 1992. The inner nuclear membrane protein p58 associates in vivo with a p58 kinase and the nuclear lamins. *EMBO (Eur. Mol. Biol. Organ.) J.* 11:4027–4036.
Smith, S., and G. Blobel. 1993. The first membrane spanning region of the lamin B receptor is sufficient for sorting to the inner nuclear membrane. *J. Cell Biol.* 120:631–637.
Soullam, B., and H.J. Worman. 1993. The amino-terminal domain of the lamin B receptor is a nuclear envelope targeting signal. *J. Cell Biol.* 120:1093–1100.
Soullam, B., and H.J. Worman. 1995. Signals and structural features involved in integral membrane protein targeting to the inner nuclear membrane. *J. Cell Biol.* 130:15–27.
Stick, R., B. Angres, C.F. Lehner, and E.A. Nigg. 1988. The fates of chicken nuclear lamin proteins during mitosis: evidence for a reversible redistribution of lamin B_2 between inner nuclear membrane and elements of the endoplasmic reticulum. *J. Cell Biol.* 107:397–406.
Torrisi, M.R., L.V. Lotti, A. Pavan, G. Migliaccio, and S. Bonatti. 1987. Free diffusion to and from the inner nuclear membrane of newly synthesized plasma membrane glycoproteins. *J. Cell Biol.* 104:733–737.
Torrisi, M.R., M. Cirone, A. Pavan, C. Zompetta, G. Barile, L. Frati, and A. Faggioni. 1989. Localization of Epstein-Barr virus envelope glycoproteins on the inner nuclear membrane of virus-producing cells. *J. Virol.* 63:828–832.
Vigers, G.P.A., and M.J. Lohka. 1991. A distinct vesicle population targets membranes and pore complexes to the nuclear envelope in Xenopus eggs. *J. Cell Biol.* 112:545–556.
Wasserman, W.J., and L.D. Smith. 1978. The cyclic behavior of a cytoplasmic factor controlling nuclear membrane breakdown. *J. Cell Biol.* 78:R15–R22.
Waterman-Storer, C.M., J.W. Sanger, and J.M. Sanger. 1993. Dynamics of organelles in the mitotic spindles of living cells: membrane and microtubule interactions. *Cell Motil. Cytoskeleton.* 26:19–39.
Wey, C.-L., M. Edidin, and R.A. Cone. 1981. Lateral diffusion of rhodopsin in photoreceptor cells measured by fluorescence photobleaching and recovery. *Biophys. J.* 33:225–232.
Wiese, C., and K.L. Wilson. 1993. Nuclear membrane dynamics. *Curr. Opin. Cell Biol.* 5:387–394.
Wilson, K.L., and C. Wiese. 1996. Reconstituting the nuclear envelope and the endoplasmic reticulum in vitro. *Semin. Cell Dev. Biol.* 7:487–496.
Worman, H.J., J. Yuan, G. Blobel, and S.D. Georgatos. 1988. A lamin B receptor in the nuclear envelope. *Proc. Natl. Acad. Sci. USA.* 85:8531–8534.
Worman, H.J., C.D. Evans, and G. Blobel. 1990. The lamin B receptor of the nuclear envelope inner membrane: a polytopic protein with eight potential transmembrane domains. *J. Cell Biol.* 111:1535–1542.
Ye, Q., I. Callebaut, A. Pezhman, J.-C. Courvalin, and H.J. Worman. 1997. Domain-specific interactions of human HP1-type chromodomain proteins and inner nuclear membrane protein LBR. *J. Biol. Chem.* 272:14983–14989.
Ye, Q., and H.J. Worman. 1994. Primary structure analysis and lamin B and DNA binding of human LBR, an integral protein of the nuclear envelope inner membrane. *J. Biol. Chem.* 269:11306–11311.
Ye, Q., and H.J. Worman. 1996. Interaction between an integral protein of the nuclear envelope inner membrane and human chromodomain proteins homologous to Drosophila HP1. *J. Biol. Chem.* 271:14653–14656.
Zatespina, O.V., V.Y. Polyakov, and Y.S. Chentsov. 1977. Some structural aspects of the fate of the nuclear envelope during mitosis. *Cytobiology.* 16:130–144.
Zeligs, J.D., and S.H. Wollman. 1979. Mitosis in rat thyroid epithelial cells in vivo. *J. Ultrastruct. Res.* 66:53–77.